Proc. Natl. Acad. Sci. USA
Vol. 79, pp. 5896–5900, October 1982
Biophysics

DNA motions in the nucleosome core particle

(triplet state anisotropy decay/methylene blue/tetrabromorhodamine 123)

J. WANG*, M. HOGAN*, AND R. H. AUSTIN†

*Department of Biochemical Sciences and †Department of Physics, Princeton University, Princeton, New Jersey 08544

Communicated by Walter Kauzmann, June 7, 1982

ABSTRACT **We have used time-resolved triplet state anisotropy decay techniques to measure the conformational flexibility of DNA in the nucleosome. From these measurements we conclude that, in a nucleosome, the DNA helix experiences substantial internal flexibility, which occurs with a time constant near 30 nsec. We find that our data can be fit well by a modified version of the Barkley–Zimm model for DNA motion, allowing only DNA twisting motions and the overall tumbling of the nucleosome. That fit yields a calculated torsional rigidity equal to 1.8×10^{-19} erg·cm, a value equal to that measured for uncomplexed DNA. We conclude from such similarity that large, fast twisting motions of the DNA helix persist, nearly unaltered, when DNA is wrapped to form a nucleosome.**

The nucleosome, the basic structural unit of eukaryotic chromatin, consists of 146 base pairs (bp) of DNA helix complexed with an octamer of histones (H3, H4, H2A, and H2B). The structure of the nucleosome has been studied extensively. As revealed by low-resolution x-ray diffraction (1) and low-angle neutron scattering (2), the nucleosome can be described as a stubby cylinder with radius of 55 Å and length of 60 Å. The DNA helix wraps around the octamer core to form approximately 1¾ turns of left-handed superhelix.

The thermal stability and conformation of the nucleosome are known to be affected by solvent conditions and temperature (3); however, very little is known about the dynamic properties of the nucleosome.

Earlier, we showed that triplet state anisotropy decay can be used to monitor nanosecond time scale twisting motions that occur in the DNA helix (4). DNA motions of this kind have been detected by using NMR (5, 6), fluorescence anisotropy decay (7–9), and ESR techniques (10) and are of considerable interest because such motions are a direct measure of the elasticity of DNA structure and because large-amplitude conformational flexibility is sure to affect the specific binding of proteins.

Because in eukaryotes most DNA exists as a nucleosome complex in chromatin, it is of importance to understand the internal flexibility of nucleosomal DNA. On the basis of ^{31}P NMR measurements, Klevan *et al.* (11) suggested that a large motion with a time constant near 1 nsec occurs in the phosphate backbone of DNA in the nucleosome. On the basis of more extensive ^{31}P relaxation measurements Shindo and McGhee (12) came to similar conclusions concerning DNA motion; their best fit to the data suggested that the phosphate backbone expresses motions in the nucleosome with time constants nearer to 30 nsec. However, on the basis of ^{1}H NMR linewidth measurements, Feigon and Kearns (13) concluded that DNA is in fact held rigidly in the nucleosome. Because of such controversy in the interpretation of NMR data, we have chosen to study DNA conformational flexibility by using triplet anisotropy decay, a technique that can measure motion over a very wide time range.

Here, we describe time-dependent triplet state anisotropy measurements of the nucleosome core particle, tagged with two different DNA specific probes, methylene blue (MB) and tetrabromorhodamine 123 (R123-B), a dye that we have synthesized for this purpose. As will be shown, both dyes bind to DNA by intercalating between base planes in the helix. However, the two dyes differ in size by nearly a factor of 2, hence we expect that any wobbling of the dye label at its DNA binding site would be frozen out in the large dye (R123-B) or at least greatly reduced in amplitude.

Using this technique, we have been able to resolve both the slow overall tumbling motion of the nucleosome and faster internal motions of the dye probes. We show that the slow rotational motion serves as an accurate measure of the size of the nucleosome in solution, and that, in addition, the dye probes do monitor large nanosecond internal motions, which probably result from fast fluctuations of DNA geometry that occur within the native structure of the nucleosome.

MATERIALS AND METHODS

Chicken blood was purchased from Pel-Freeze. Packed erythrocytes were stored at −70°C, thawed, and then washed twice with 150 mM NaCl/15 mM cacodylic acid/0.1 mM phenylmethylsulfonyl fluoride, pH 7.2. Nuclei were isolated by washing with the same buffer containing 0.25% Nonidet P-40, then washed twice again with the same buffer to remove detergent. The nuclei were suspended in 10 mM 1,4-piperazinediethanesulfonic acid/170 mM KCl/11% sucrose/3 mM $CaCl_2$/0.1 mM cacodylic acid/0.1 mM phenylmethylsulfonyl fluoride, pH 7.0. Micrococcal nuclease (Sigma) was added directly to these nuclei at a ratio of 0.4 unit/mg of nuclear DNA. After 7 min of digestion at 37°C, the reaction was stopped by cooling to 4°C and adding Na_2EDTA to 10 mM. The digestion solution was centrifuged at 15,000 × *g* for 3 min.

The resulting supernatant was fractionated at 4°C on a Sepharose 4B gel column (Pharmacia), eluting with 10 mM Tris·HCl/1 mM Na_2EDTA/0.1 mM phenylmethylsulfonyl fluoride, pH 7.5. Nucleosomes were concentrated and refractionated by preparative gel electrophoresis at 4°C over a 2.6% acrylamide/0.1% bisacrylamide column (Savant), eluting with 90 mM Tris borate/2.5 mM Na_2EDTA, pH 8.0.

The purities of nucleosomes and uncomplexed DNA fragments have been assayed by monitoring their electrophoretic mobilities on 5% acrylamide gels, relative to DNA size markers (*Hae* III digest of phage φX174 replicative form DNA). The protein composition of the nucleosomes was assayed by measuring protein electrophoresis on 15% acrylamide/sodium dodecyl sulfate gels. The physical state of nucleosome samples was also checked by performing a partial DNase I digestion of ^{32}P-labeled nucleosomes, as described by Lutter (14).

MB was purchased from Eastman Kodak and was further

The publication costs of this article were defrayed in part by page charge payment. This article must therefore be hereby marked "*advertisement*" in accordance with 18 U. S. C. §1734 solely to indicate this fact.

Abbreviations: bp, base pair(s); MB, methylene blue; R123-B, tetrabromorhodamine 123.

purified by chromatography over Sephadex LH-20 (Pharmacia), eluting with methanol. Rhodamine 123 was purchased from Eastman Kodak, then brominated by a procedure described by Cherry for the synthesis of eosin (15). The composition of the rhodamine dye has been assayed by NMR, mass spectroscopy, elemental analysis and osmotic molecular weight determination (Galbraith Laboratories, Knoxville, TN). On the basis of that analysis we conclude that the dye resulting from this procedure is pure tetrabromorhodamine 123 chloride.

DNA concentration was determined spectrophotometrically, using $\varepsilon_{258} = 1.3 \times 10^4\ M^{-1}\ cm^{-1}$ (M referring to bp) for both free and nucleosomal DNA. Dye concentrations were determined by using $\varepsilon_{507} = 5.0 \times 10^4\ M^{-1}\ cm^{-1}$ for R123-B, $\varepsilon_{665} = 4.4 \times 10^4\ M^{-1}\ cm^{-1}$ for MB.

Fluorescence measurements were made on a Perkin Elmer MPF-4 spectrofluorometer. Linear dichroism measurements were performed as described previously (16) on a device made available by D. M. Crothers (Department of Chemistry, Yale University).

Triplet anisotropy decay measurements were made on a device similar to that which we have described elsewhere (4). As in our earlier work, we have monitored optical anisotropy of the depleted singlet state, rather than the triplet state directly (see ref. 17 for a discussion of the method). For MB, the excitation source was the polarized emission from a rhodamine 640 dye laser (λ = 604 nm) pumped by a frequency-doubled Nd:YAG pulsed laser (Molectron MY-32; Molectron Corp., Sunnyvale, CA). For R123-B, the doubled Nd-YAG source (λ = 532 nm) was used directly. The laser was operated at 10 Hz with an average energy of 0.7 mJ per pulse and a pulse width of 15 nsec. For MB, the monitoring beam was produced by a linearly polarized HeNe laser (λ = 632.8 nm). For R123-B, the monitoring beam was produced by an argon laser (λ = 514 nm).

RESULTS

In Fig. 1 *Left* we show acrylamide gels of the sort we have used to characterize the material used in this work. As shown by their mobility on 5% acrylamide gels, both the intact nucleosome and its DNA component are monodisperse. By reference to DNA size standards we calculate that, as expected, the DNA component of the nucleosomes is 146 ± 2 bp long. As can be seen in Fig. 1 *Right*, the protein component of these nucleosomes is composed of nearly equimolar amounts of histones H3, H2B, H2A, and H4, and is free from detectable amounts of H1, H5, or any nonhistone protein. The phasing of DNA when wrapped on these nucleosomes has been checked by performing a partial DNase I digestion of nucleosomes labeled at the 5′ DNA end with ^{32}P as described by Lutter (14). The resulting digests show a 10-bp DNA repeat and intensity distribution similar to that described for nucleosomes by Lutter (not shown).

DNA extracted from these nucleosomes migrates as a sharp band on denaturing 2% agarose/0.05 M NaOH gels (not shown). On the basis of such protein and DNA mobilities, we conclude that nucleosome DNA in these experiments is free from internal nicks, and that the nucleosome core particles used in this work are monodisperse with respect to protein composition and DNA length.

Because we are using MB and R123-B as dye probes, it is crucial that we understand in detail the mechanism by which they bind to DNA and to nucleosomes. As we have shown elsewhere (4), MB binds to DNA by intercalating into the helix. We have measured the properties of this intercalated complex with 146-bp nucleosome DNA and have summarized those results in Table 1. As seen in Table 1, when bound to 146-bp DNA, MB undergoes a decrease to 1/6 in fluorescence intensity, a 10-nm red shift in its absorption spectrum, and a 32% decrease in its extinction coefficient. Linear dichroism measurements show that, when bound, MB's absorption dipole is oriented at 71° relative to the helix axis. That dye orientation and those spectral changes are very similar to the values measured for other intercalating dyes (16, 18, 20, 21).

As seen in Table 1, the properties of the MB complex with the nucleosome are nearly identical to those of the complex with free DNA. However, the apparent affinity of base pairs for MB in the nucleosome (*nk*) is somewhat smaller than the value measured for DNA. As seen in Table 1, the relative linear dichroism of MB and the DNA base planes is nearly identical in the free DNA and in the nucleosome, suggesting that MB continues to bind to the nucleosome by intercalating into the DNA helix. The linear dichroism data also suggest that MB does not bind to the

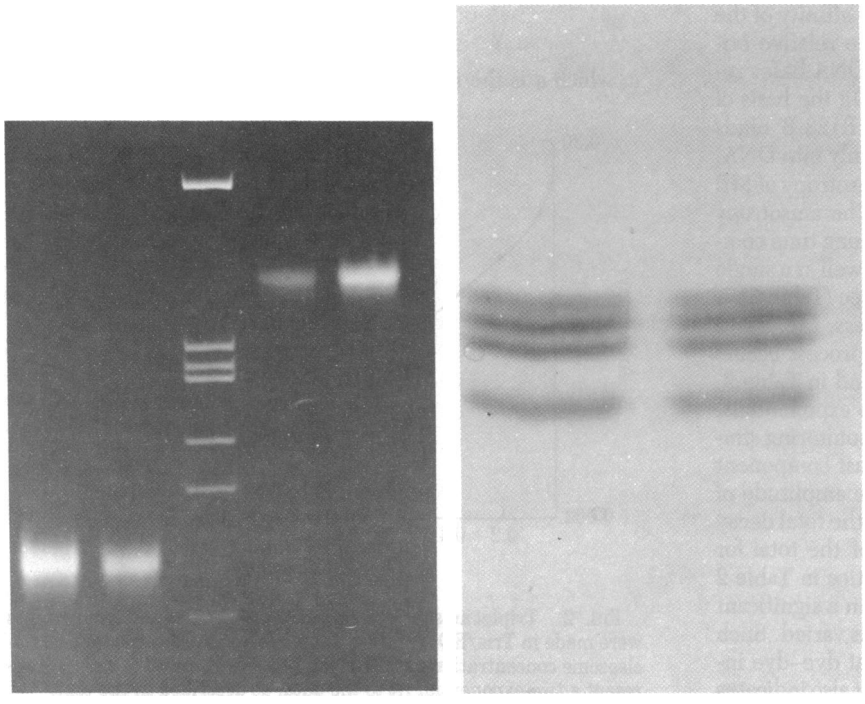

FIG. 1. Gel electrophoresis of nucleosome samples. (*Left*) A 5% acrylamide gel of the material used in this work; lanes 1 and 2 (counting from the left) correspond to DNA extracted from the nucleosome; lanes 4 and 5 correspond to the intact nucleosome particle. Lane 3 is the *Hae* III restriction endonuclease digest of ϕX174 DNA. Samples were stained with ethidium bromide. (*Right*) A 15% acrylamide/sodium dodecyl sulfate gel of histones extracted from the nucleosomes used in this work. In order of increasing mobility, the bands correspond to histones H3, H2B, H2A, and H4.

Table 1. Physical properties of MB and R123-B complexes

Complex or dye	nk,[a] $M^{-1} \times 10^{-5}$	$\frac{P(\text{dye})}{P(\text{DNA})}$[b]	α,[c] degrees	I/I_0[d]	λ_{em},[e] nm	λ_{max},[f] nm	ε,[g] $M^{-1}\,cm^{-1}$	τ, μsec With O_2[h]	τ, μsec No O_2[i]	k_q,[j] $M^{-1}\,sec^{-1}$
MB–146-bp DNA	7.5	1.0	71 ± 1	0.17	680	675	30,000	15	70	1.8×10^8
MB–nucleosome	1.5	1.05	72	0.18	680	672	30,000	4.0	34	6.6×10^8
MB in buffer	—	—	—	1	680	665	44,000	1.4	30	1.9×10^9
R123-B–146-bp DNA	4	0.80	69 ± 1	0.16	532	516	35,000	30	78	9×10^7
R123-B–nucleosome	0.3	0.72	67 ± 1	0.20	535	513	34,000	5.8	40	4.5×10^8
R123-B in buffer	—	—	—	1	530	507	50,000	2.2	33	1.2×10^9

[a] nk refers to the apparent binding constant of the dye measured at 5°C in 10 mM Tris·HCl/0.05 mM Na_2EDTA buffer, pH 7.8 (Tris/EDTA buffer). Binding isotherms were calculated from a titration of the dye with a concentrated solution of DNA or nucleosomes, monitoring the fluorescence change occurring on binding. Data were analyzed using standard techniques (18). nk was measured by a linear extrapolation of a Scatchard plot of the data. As mentioned in the text, nk is measured in bp concentration units.

[b] Ratio of dye linear dichroism to linear dichroism of DNA in the complex at 265 nm. MB dichroism was measured at 620 nm. R123-B dichroism was measured at 507 nm. Measurements of linear dichroism with 146-bp DNA were made in ⅓ × Tris/EDTA buffer; measurements made with nucleosomes were made in Tris/EDTA buffer.

[c] Orientation of the dye absorption dipole relative to the helix axis at the dye binding site. α was calculated from data with nucleosomes by using methods described elsewhere (19).

[d] Fluorescence decrease on binding. Measurements are made at the excitation and emission wavelength maxima of the unbound dyes in Tris/EDTA.

[e] Fluorescence emission maximum.

[f] Absorption maximum.

[g] Extinction coefficient at the absorption maximum.

[h] Triplet state lifetime in air-saturated solution.

[i] Triplet state lifetime in argon-saturated solution.

[j] Bimolecular quenching constant for O_2 quenching of the dye triplet state.

ends of the helix in the nucleosome because such specific binding would lead to averaged dichroism for MB, which would be much larger than the (solenoidally averaged) value measured for the base planes in the nucleosome (19).

Like MB, R123-B is a planar aromatic cation with a structure similar to other known intercalating drugs and dyes. As shown in Table 1, the optical changes that occur when R123-B binds to DNA are very similar to those seen for MB: a decrease to ⅙ in fluorescence, a 9-nm red shift, and a 31% decrease in extinction coefficient. Like MB, R123-B binds to DNA to form a tight complex ($nk = 4 \times 10^5\ M^{-1}$) with its optical transition moment oriented at 69° relative to the helix axis. On the basis of these similarities we conclude that R123-B also intercalates into DNA. As for MB, the absorbance and fluorescence properties of its nucleosome complex are similar to those with DNA alone. As with MB, there is a modest drop in the affinity of the dye for DNA base pairs in the nucleosome. The relative orientation of the dye transition moment and the DNA bases remains the same in DNA and the nucleosome. On the basis of these similarities we conclude that, like MB, R123-B binds tightly to the nucleosome by intercalating randomly into DNA.

In Fig. 2 and 3 we show the decay of triplet anisotropy of MB and R123-B complexes with the nucleosome. The anisotropy decays as the sum of at least two processes. The long time component of this decay for both dyes can be fit very well as a single exponential with a time constant of 370 ± 20 nsec (Table 2).

In addition to the slow anisotropy decay process, Fig. 2 and 3 show that an additional fast anisotropy decay process occurs in the nucleosome. As shown in Figs. 2 and 3 and in Table 2, when such decay curves are fit to a sum of two exponentials, it appears from those fits that the two dyes are monitoring similar decay processes: the time constant for the fast component of anisotropy decay is 35 nsec for both dyes; the amplitude of the fast decay process amounts to 50% ± 10% of the total decay for MB-tagged nucleosomes and 37% ± 20% of the total for those tagged with R123-B. It is important to notice in Table 2 that the anisotropy decay curves do not change in a significant way as the number of dye labels per nucleosome is varied. Such independence is important because it shows that dye–dye interactions do not contribute to anisotropy decay. It also indicates that at the low binding densities that we have employed dye binding does not alter nucleosome conformation.

DISCUSSION

The chromophores whose motion we measure are intercalated into the DNA. If the attractive forces between the DNA and histone core are strong enough, then any internal motion of the DNA would be stopped and the dye labels would in effect be attached to a rigid body. The expected anisotropy decay for a rigid ellipsoid has been solved and consists of three exponentials (22). For stubby ellipsoids (such as a nucleosome) the three time constants will be nearly degenerate in time (22). Consequently it is adequate for our purposes to model the nucleosome as a sphere with an effective radius r_{eff}:

$$\frac{4}{3}\pi r_{eff}^3 = \pi a^2 b, \qquad [1]$$

in which a is the radius of the (nearly cylindrical) nucleosome

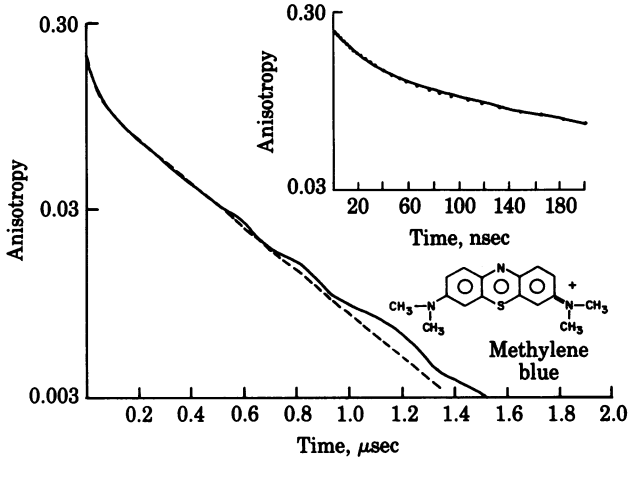

FIG. 2. Triplet anisotropy decay of the nucleosome. Measurements were made in Tris/EDTA buffer at 5°C. MB-labeled nucleosomes, nucleosome concentration (bp) 770 μM; MB = 11 μM. ––– and ····· represent a two-exponential fit to the data, as described in the text.

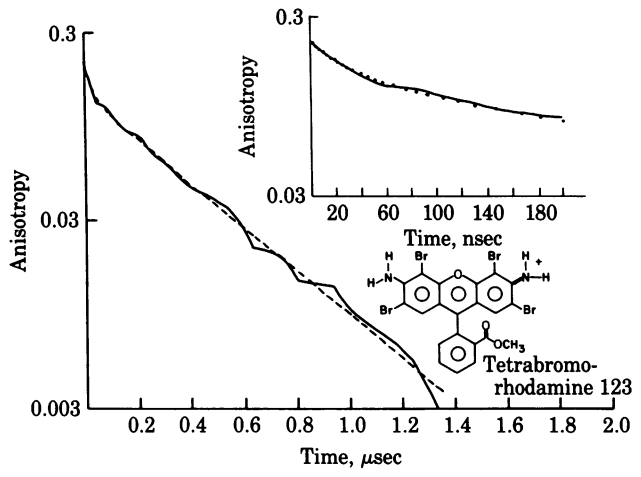

FIG. 3. R123-B-labeled nucleosomes; nucleosome concentration (bp), 1,500 μM; R123-B = 18 μM. Experimental conditions and symbols are as in Fig. 2.

and b is its height. The anisotropy decay $r(t)$ predicted for a *rigid* nucleosome then is (22):

$$r(t) = r(0)e^{-6Dt} \quad [2]$$

in which

$$6D = \frac{3k_BT}{4\pi r_{eff}^3\eta} = \frac{1}{\tau_{rot}}, \quad [3]$$

in which k_B is the Boltzmann constant, T is the absolute temperature, and η is the medium viscosity in poise. The longest measured decay time for both MB- and R123-B-tagged nucleosomes (0.37 μsec) yields, by this analysis, r_{eff} = 60 Å. This value for the effective radius is nearly identical to values measured previously for the nucleosome (19) and is in good agreement with its expected hydrated dimensions (1).

As Barkley and Zimm (23) and Schurr and co-workers (8) have discussed theoretically, it is possible to model the motion of DNA by assuming that it has both torsional and bending degrees of freedom. Barkley and Zimm showed that if no bending occurs the anisotropy should decay as:

$$r_T(t) = (0.1)(3p^2 - 2)^2 + 0.3p^2e^{-\Gamma} + 1.2p^2(1 - p^2)e^{-\Gamma/4}, \quad [4]$$

in which p is the sine of the angle the dipole moment makes with the helix axis and Γ is the twisting decay function:

$$\Gamma(t) = 4k_BT\left(\frac{t}{\pi c\rho}\right)^{1/2}, \quad [5]$$

in which

$$\rho = 4\pi\eta b^2. \quad [6]$$

Here c is the torsional rigidity and b is the (hydrated) radius of the DNA duplex.

As a first model for DNA motion in the nucleosome, we propose that when wrapped onto the nucleosome DNA can twist but not bend due to the constraint of being on the protein surface. When wrapped in this fashion the helix will also experience the overall motion of the complex, so we imagine that, in total, DNA motion will consist of a fast twist superimposed on the (slower) overall motion of the nucleosome. Our final expression for such DNA motion is:

$$r_N(t) = r_T(t)\,(e^{-t/\tau_R}), \quad [7]$$

in which τ_R is the global, averaged rotational time of the nucleosome as defined in Eq. 3, and $r_T(t)$ is the twist function (Eq. 4) defined by Barkley and Zimm (23).

In Fig. 4 we have compared the theoretical anisotropy decay to the observed decay for MB-tagged nucleosomes. We have chosen b to be 13 Å, in agreement with our earlier work (4), and have determined c (torsional rigidity) to be best fit by 1.8×10^{-19} erg·cm (1 erg·cm = 10^{-9} J·m), as is shown in the *Inset* to Fig. 4. This value of torsional rigidity also gives best fits, using Barkley–Zimm theory, to the anisotropy decay of pBR322 plasmid DNA (unpublished data).

Note that in Fig. 4, the data at long times are fit best by a decay time equal to 0.45 μsec rather than 0.37 μsec (the best fit to a sum of two exponentials). Such a difference corresponds to an effective radius equal to 65 Å rather than 60 Å (Eq. 2 and 3). It is difficult to choose between these two values for the effective nucleosome radius because of their similarity and because of ambiguity inherent in hydrodynamic model building. Either is qualitatively consistent with the hydrated dimensions of a nucleosome (1). As seen in Fig. 4, the amplitude of anisotropy decay at long times is 10–20% larger than predicted by our simple motional model. However, considering the simplicity of the model, we feel that such a discrepancy is small and that our anisotropy decay data are well described by this modified Barkley–Zimm analysis.

We are led by this analysis to the important conclusion that the torsional rigidity of DNA complexed in intact nucleosomes

Table 2. Anisotropy decay of MB and R123-B complexes

Complex		Dye molecules								
DNA	Dye	bound[a]	r_1	τ_1, nsec	r_2	τ_2, nsec	r_3	τ_3, μsec	r_0[b]	R[c]
146-bp DNA	MB	1.5	0.11	50	0.055	290	0.03	3.2	0.20	
Nucleosome	MB	0.6	0.11	36	0.11	417			0.22	0.5
Nucleosome	MB	2.2	0.11	30	0.11	380			0.22	0.5
146-bp DNA	R123-B	1.5	0.13	70	0.06	320	0.03	3.5	0.20	
Nucleosome	R123-B	0.6	0.08	29	0.14	370			0.22	0.4

Experimental conditions are precisely as described for Fig. 2. Anisotropy decay data from dye complexes with 146-bp DNA were fit to a sum of three exponential processes with amplitudes r_1, r_2, and r_3 and decay times τ_1, τ_2, and τ_3. Anisotropy decay data for nucleosomes were fit within experimental accuracy to a sum of two exponentials.

[a] The number of dye label molecules bound per macromolecule; i.e., 1.0 means one dye bound per nucleosome or 146-bp DNA fragment.

[b] r_0 is the measured anisotropy at the earliest measurable time (2 ns) and is equal to Σr_i. r_0 is equivalent to the intrinsic anisotropy in the limit that substantial decay does not occur during the first 2 ns.

[c] R is the fraction of the total anisotropy arising from the fast decay component and is equal to $r_1/(r_1 + r_2)$.

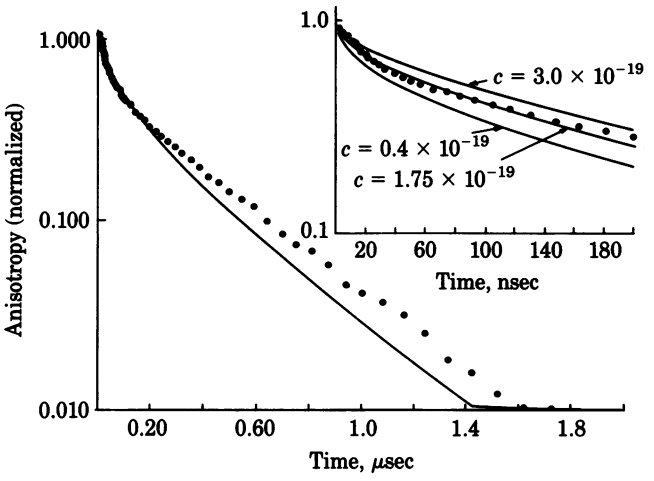

FIG. 4. MB-labeled nucleosome anisotropy decay data compared with the theoretical prediction of Eqs. 4–9. We have renormalized our data (●) to yield an initial anisotropy of 0.40. The validity of this approach has been discussed in ref. 4. We have chosen τ_{rot} to be 450 nsec in order to get a best fit to the data. (*Inset*) Data on an expanded scale and theoretical curves for three different torsional rigidities (——). As discussed, the data are best fit by a torsional rigidity c of 1.75×10^{-19} erg·cm.

is quite similar to the torsional rigidity of a free DNA helix.

One possible artifact in these measurements is wobbling of the intercalated dye within its DNA binding site, independent of any motion of the DNA itself. In other words, our data can be explained by two models: (*i*) The dyes bind to DNA in the nucleosome but, when intercalated, are free to move about inside the DNA binding site. (*ii*) The dyes are held firmly at the DNA binding site, while the DNA helix itself experiences fast fluctuations in its structure.

Although it is impossible to rule out unambiguously a (trivial) motion of the dye inside its binding site, we favor the second explanation for several reasons:

(*i*) R123-B is much larger than MB, yet monitors the same fast motions. Although MB and R123-B appear to intercalate in similar ways into DNA, it is important to remember that the two dyes have very different structures. In particular, the size of the R123-B ring system has been increased substantially by adding four bromines (each is nearly as large as a methyl group) and a benzene substituent at position 2 that is nearly perpendicular to the aromatic ring system. When the dyes are intercalated, wobbling motions within the binding site, if they occur, should be very sensitive to the size and pattern of substitution of the bound dye molecule; if MB experiences wobbling motions at its binding site then those motions should be greatly reduced in the R123-B complex (because R123-B is much larger). Quite the opposite, the experimental decay curves for MB and R123-B complexes are identical, within experimental accuracy (Figs. 2 and 3), which implies that the bulky substituents of R123-B have no effect on the motion being monitored. Such constancy of the measured fast component is strong evidence against wobbling.

(*ii*) Nanosecond time scale DNA motions have also been detected in the phosphate backbone of nucleosome DNA by using ^{31}P NMR techniques (11). The magnitude and time scale of such phosphate motions are qualitatively similar (in amplitude and time scale) to the kind of nucleosome motions we have described here and to the fastest components of DNA motion measured in uncomplexed DNA by using ^{31}P NMR (5, 6, 11), fluorescence anisotropy decay (7, 9, 10), phosphorous anisotropy decay (4), and ESR techniques (10).

CONCLUSIONS

We have used triplet anisotropy decay techniques to measure the motion of dyes intercalated into nucleosome-complexed DNA. Two dyes with different steric constraints (MB and a brominated rhodamine 123) were used to discriminate dye wobbling from accurate measurement of DNA motion.

We have found that DNA, when bound to the histone core, experiences large and fast local motion. This motion can be quite accurately fit by use of the Barkley and Zimm model for DNA motions (23), allowing only for local twisting motions of the helix and the overall rotational motion of the nucleosome. The data are best fit with a torsional rigidity c of $1.8 \pm 1.0 \times 10^{-19}$ erg·cm, a value nearly identical to that measured for free DNA. Within the context of this simple model we conclude that fast fluctuations of helix twist persist, nearly unaltered, when DNA is wrapped to form a nucleosome.

Although the triplet state anisotropy decay method has limitations (a dye probe is required) when considered with other techniques for measuring DNA flexibility, together they point out that large, fast conformation fluctuations may be intrinsic to the structure of DNA. In the context of such mounting evidence, we believe that it is now necessary to reconsider existing models for DNA conformation and protein binding in terms of models that allow for substantial fluctuation of helix geometry.

We thank N. Dattagupta for his help with linear dichroism measurements, C. Monitto for both construction of apparatus for the laser experiments and assistance in measurements, and J. Karohl for helpful discussions. This work was supported by National Institutes of Health Grant GM 2904701 and American Cancer Society Grant NP352.

1. Finch, J. T., Lutter, L. C., Rhodes, D., Brown, R. S., Rushton, B., Levitt, M. & Klug, A. (1977) *Nature (London)* **269**, 29–36.
2. Hjelm, R. P., Kneale, G. G., Suau, P., Baldwin, J. R., Bradbury, E. M. & Ibel, K. (1977) *Cell* **10**, 139–151.
3. Weischet, W. O., Tatchell, K., Van Holde, K. E. & Klump, K. (1978) *Nucleic Acids Res.* **5**, 139–159.
4. Hogan, M., Wang, J., Austin, R. H., Monitto, C. L. & Hershkowitz, S. (1982) *Proc. Natl. Acad. Sci. USA* **79**, 3518–3522.
5. Bolton, P. H. & James, T. L. (1979) *J. Am. Chem. Soc.* **102**, 25–31.
6. Hogan, M. & Jardetzky, O. (1979) *Proc. Natl. Acad. Sci. USA* **76**, 6341–6345.
7. Millar, D. P., Robbins, R. J. & Zewail, A. H. (1980) *Proc. Natl. Acad. Sci. USA* **77**, 5593–5597.
8. Thomas, J. C., Allison, S. A., Appelldof & Schurr, J. M. (1980) *Biophys. Chem.* **12**, 177–188.
9. Wahl, P., Paoletti, J. & LePecq, J. B. (1980) *Proc. Natl. Acad. Sci. USA* **65**, 417–421.
10. Robinson, B. H., Lerman, L. S., Beth, A. H., Frisch, H. L., Dalton, L. R. & Auer, C. (1980) *J. Mol. Biol.* **139**, 19–44.
11. Klevan, L., Armitage, I. M. & Crothers, D. M. (1979) *Nucleic Acids Res.* **6**, 1607–1616.
12. Shindo, H. & McGhee, J. D. (1980) *Biopolymers* **19**, 523–537.
13. Feigon, J. & Kearns, D. R. (1979) *Nucleic Acids Res.* **6**, 2327–2333.
14. Lutter, L. C. (1978) *J. Mol. Biol.* **124**, 391–420.
15. Cherry, R. J., Cogoli, A., Oppliger, M., Schneider, G. & Semenza, G. (1976) *Biochemistry* **15**, 3653–3656.
16. Hogan, M., Dattagupta, N. & Crothers, D. M. (1979) *Biochemistry* **18**, 280–288.
17. Cherry, R. J. (1978) *Methods Enzymol.* **54**, 47–61.
18. LePecq, J. B. & Paoletti, C. (1967) *J. Mol. Biol.* **27**, 87–106.
19. Crothers, D. M., Dattagupta, N., Hogan, M., Klevan, L. & Lee, K. S. (1978) *Biochemistry* **17**, 4523–4525.
20. Weill, G. & Calvin, M. (1963) *Biopolymers* **1**, 101–117.
21. Wu, H. M., Dattagupta, N., Hogan, M. & Crothers, D. M. (1980) *Biochemistry* **19**, 626–634.
22. Tao, T. (1969) *Biopolymers* **8**, 609–632.
23. Barkley, M. D. & Zimm, B. H. (1979) *J. Chem. Phys.* **70**, 2991–3007.